

LOW-THRUST MULTIPLE GRAVITY ASSIST MISSIONS

Ghanghoon Paik*, Robert G. Melton[†]

The application of continuous low thrust to a gravity assist can result in extra gain of Δv after the maneuver. In this paper, low thrust is applied to a gravity assist maneuver around Venus to evaluate possible benefits. Particle swarm optimization is applied to find the optimal sphere-of-influence entry location and the thrust direction and magnitude. Once the full trajectory is determined, the characteristics of both free and thrust gravity assists are compared to evaluate the benefit of additional thrust over free gravity assist. Thrusted maneuvers show improvement in Δv gain and closer approach to a planet.

INTRODUCTION

Gravity assist maneuvers are widely used for deep space missions to utilize benefits from free Δv and obtain opportunities to swing-by planetary bodies at close distance. Additional thrust at the periapsis of the trajectory is known to boost the effect of Δv gain of the gravity assist (Oberth effect).¹ In order to get maximum benefit from the thrust, it should be placed at the periapsis where orbital velocity is maximized. A spacecraft can thrust at periapsis of either an elliptical transfer orbit or hyperbolic flyby trajectory inside a planet sphere-of-influence (SOI) as shown in Figure 1.

Previous research has combined gravity assist with thrust. Some work analyzed the effect of the Oberth effect when impulsive thrust is applied at the periapsis of an elliptical trajectory similar to Figure 1a.^{2,3} These approaches show potential benefits of propulsion added to free gravity assist. Also, multiple gravity assists with deep space maneuvers (DSMs) is an active research area. Research done in this field has implemented impulsive or continuous thrust during the coasting phase of interplanetary missions.⁴⁻¹¹ Applied DSMs allow a spacecraft to encounter a target planet at a desired time. DSMs can also be used to increase the energy of an orbit or change the direction of the spacecraft.

In this work, gravity assist combined with the Oberth effect using low thrust is used to show the behaviors and benefits for multiple gravity assist missions. Also, progress on a sequence search method is discussed. The patched conic assumption is made to simplify the trajectory calculation of a spacecraft. Continuous low thrust is applied during the flyby phase inside the SOI as shown in Figure 1b.

METHODS

Methods used in the preliminary work are covered here including dynamics, sequence searching, and particle swarm optimization.

*PhD candidate, Department of Aerospace Engineering, Pennsylvania State University, University Park, PA 16802

[†]Professor, AAS Fellow, AIAA Associate Fellow, Department of Aerospace Engineering, Pennsylvania State University, University Park, PA 16802

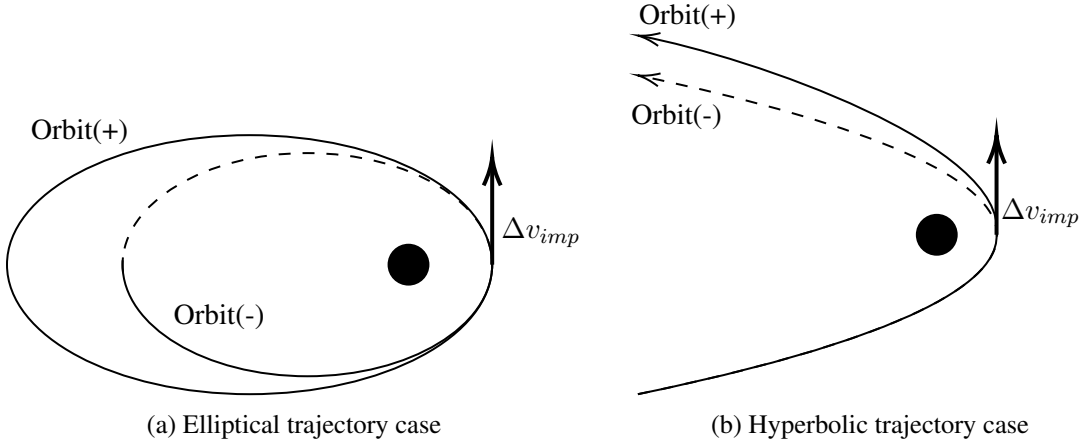


Figure 1: Oberth effect with impulsive Δv

The dynamics of a spacecraft is based on simple two-body equations in polar coordinates and thrust is applied for low powered gravity assist. In this paper, searching for the gravity assist sequence is not completed. However, it is still in development for the future application. One of the highly considered techniques, the Δv isoline graphical method, is described. The use of Δv isoline graphical method may reduce complexity of sequence search for multiple gravity assist mission design. The particle swarm optimization method is implemented to find an optimal amount and direction of thrust.

Dynamics

In this work, all orbits are assumed to be 2-D coplanar for simplicity. Since continuous thrust is applied while a spacecraft is flying inside the SOI, the behavior of the spacecraft should be determined for both conditions (with and without applied thrust) to represent the effect of the thrust.

Due to the 2-D assumption, the spacecraft dynamics can be represented in a polar coordinate form. The heliocentric axis is based on the J2000 ecliptic plane and the planetocentric axis is pointing in the same direction as the heliocentric axis but fixed to the planet.^{12,13} Let r, v_r, θ , and v_θ be radial distance, radial velocity, angular displacement from x -axis, and transverse velocity, respectively. The equation is written in state-space form as^{14,15}

$$\dot{\vec{x}} = \begin{bmatrix} v_r \\ -\frac{\mu-r}{r^2} v_\theta^2 \\ v_\theta \\ -\frac{r}{v_r} v_\theta \end{bmatrix} \quad (1)$$

for $\vec{x} = [r, v_r, \theta, v_\theta]^T$. Equation (1) is used to generate the heliocentric trajectory of the spacecraft while it is coasting from one planet to another. Then, for powered gravity assist trajectories, the thrust term is introduced. Applying thrust adds an input

$$\dot{\vec{x}} = \begin{bmatrix} v_r \\ -\frac{\mu-r}{r^2} v_\theta^2 \\ v_\theta \\ -\frac{r}{v_r} v_\theta \end{bmatrix} + \frac{T}{m} \begin{bmatrix} 0 \\ \sin \beta \\ 0 \\ \cos \beta \end{bmatrix}, \quad (2)$$

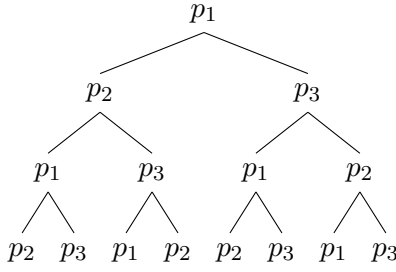


Figure 2: Sample scenario of gravity assist trajectories

where T is the thrust, m is the spacecraft mass, and β is the thrust-pointing angle. The thrust pointing angle β for the continuous thrust is defined as as third-order polynomial

$$\beta = \beta_1 + \beta_2 t + \beta_3 t^2 + \beta_4 t^3 \quad (3)$$

where the coefficients β_i are determined via a heuristic optimization method.

Searching for Sequences

It is not an easy task to find an optimal sequence for multiple gravity missions. There are several challenges to generating a (optimal) sequence. One of them is the complexity of the problem, which can increase rapidly as more planets or swing-by's are considered. If all possibilities are included, the complexity of the problem becomes $(N_{planet} - 1)^{N_{GA} + 1}$ where $N_{planets}$ is the number of planets involved and N_{GA} is the number of gravity assist maneuvers. For example, if 3 planets and 2 gravity assists maneuvers are planned to be used, the total number of possible scenarios is 2^3 . This sample scenario is represented in Figure 2. If returning to the same planet for swing-by is also considered, the complexity increases to $N_{planet}^{N_{GA} + 1}$.

Because gravity assist maneuvers can be performed only when the spacecraft encounters a planetary body, the number of possible trajectories can be reduced if unavailable ones are eliminated. In order to check the validity of the maneuver, the Δv isoline graphical method is introduced for the work. The graphical method is based upon the amount of Δv required to transfer from a circular departure planet's orbit to an elliptical transfer orbit.¹⁶⁻¹⁹ In Figure 3, \vec{r}_c represents the radius of

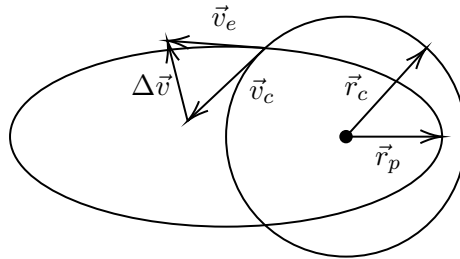


Figure 3: Impulsive Δv diagram for the circular-elliptical orbit transfer

circular orbit of the departure planet and \vec{r}_p is radius of periapsis of the elliptical transfer orbit from the Sun. Since the orbit of the planet is fixed, applying different amount of Δv changes the size of the transfer orbit. All possible cases are shown in the Figure 4. From Figure 4, the relationship between r_p and Δv can be obtained and plotted as Figure 5. By plotting such a relationship for

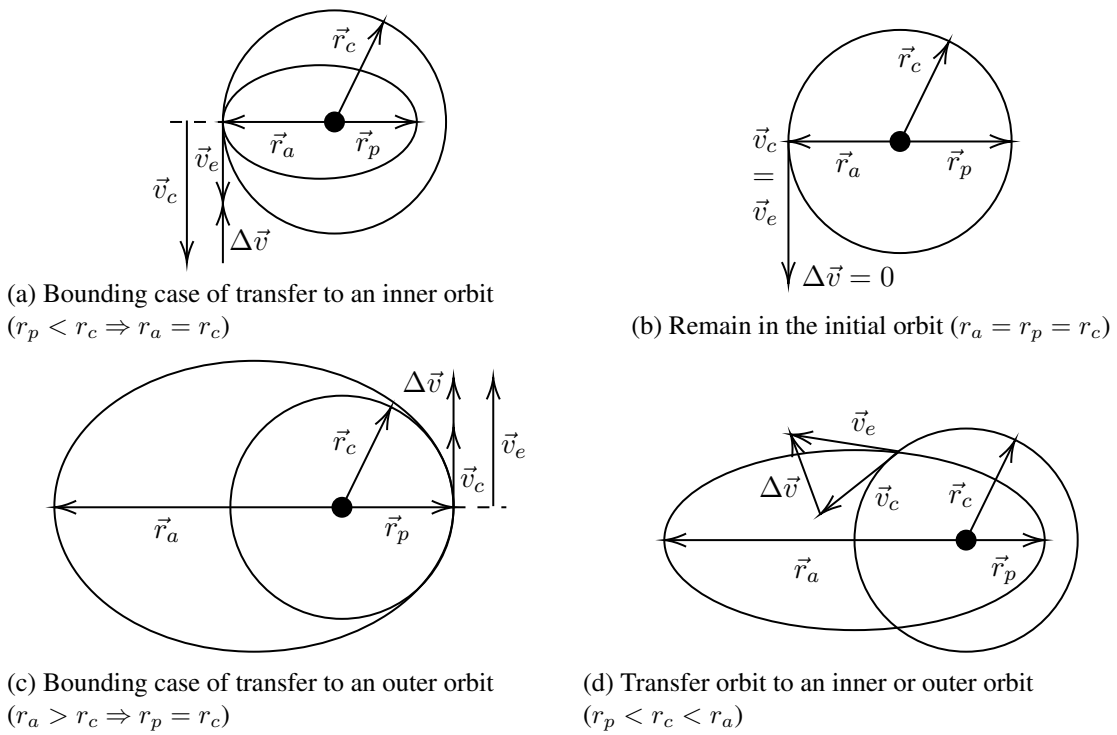


Figure 4: Four possible scenarios of transfer orbits with restraints

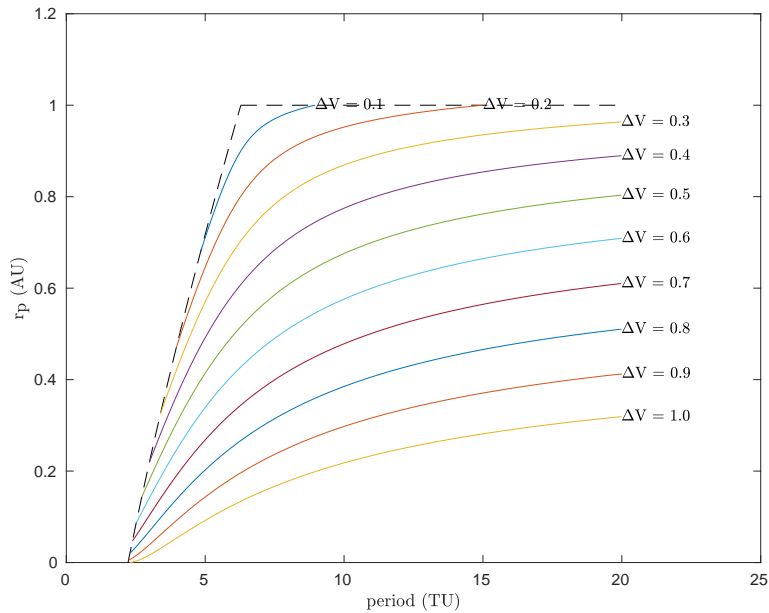


Figure 5: Isolines of periapsis distance vs. period for given Δv

multiple planets, combined isoline figures can be generated. For example, Figure 6 represents the combination of Venus and Mars plots. From the plot with multiple planets, intersections where two

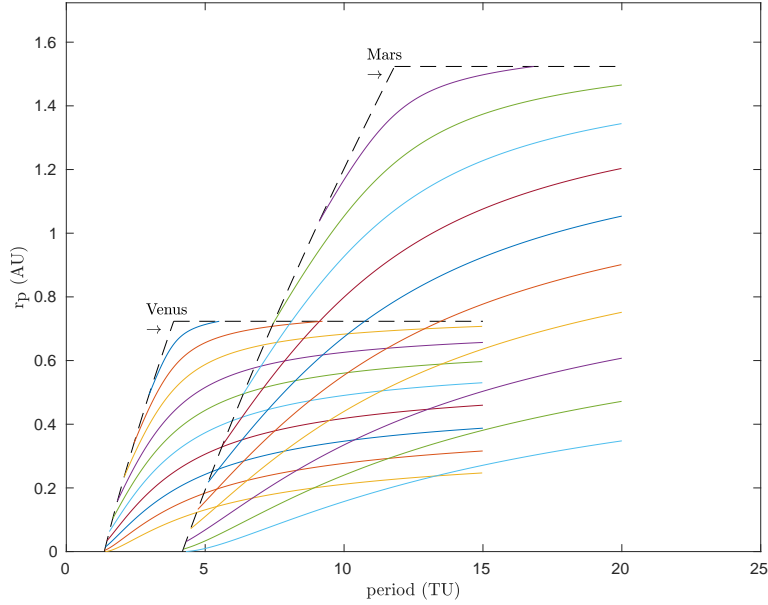


Figure 6: Isolines of Venus and Mars

lines coincide indicate characteristics of possible gravity assist transfers. Therefore, only transfers with achievable amounts of Δv 's need to be evaluated when designing a mission.

Particle Swarm Optimization for Trajectory Propagation

In this work, the PSO with inertial, cognitive, and social influences is used to find trajectories of a spacecraft both when the thrust is turned on and off inside SOI. The PSO uses five parameters, four from Equation (3) and one for thrust magnitude, to obtain maximum Δv of the gravity assist maneuver. The particle structure is

$$P = [\beta_1, \beta_2, \beta_3, \beta_4, N_{thr}] \quad (4)$$

where the β_i are polynomial coefficients of the thrust pointing angle and N_{thr} is the magnitude of thrust in Newton. The cost function, J , is the sum

$$J = |\Delta v_f| + \alpha |\Delta r_p| \quad (5)$$

where $|\Delta v_f|$ is a difference in final velocity of (with and without the applied thrust) the spacecraft when it is leaving the SOI and $|\Delta r_p|$ is a difference in periapsis distance with and without the applied thrust. The second term is a penalty function with α defined as

$$\alpha = \begin{cases} 0 & \text{if } |\Delta r_p| < 10^{-3} \\ 1000 & \text{if } |\Delta r_p| > 10^{-3} \end{cases} \quad (6)$$

This penalty term is imposed to enforce a desired periapsis distance.

PRELIMINARY RESULTS

A preliminary result that reproduces the first gravity maneuver of the Cassini mission is presented. Once a spacecraft departs from Earth, it coasts freely until it reaches an arrival planet. The coasting trajectory can be determined from Lambert's solution. While solving the Lambert's problem, it is possible to specify the SOI entry point. Choosing an optimal entry point can affect the amount of Δv gain from the swing-by. After the optimal entry point is found, continuous low thrust is applied to maximize the final Δv . Though it is not necessarily maximized, the work done here is focused on maximum Δv output.

In this work, several assumptions are made for the simulation. The predefined assumptions are: 1) Spacecraft mass is 2000 kg. 2) Maximum thrust is 10 N 3) Fuel consumption is not considered. 4) The thruster can point any direction. 5) Earth launch and Venus arrival dates are October 15, 1997 and April 26, 1998 at 00:00:00.

The inertial coordinate system used in this research is based on the 2-D ecliptic plane at the epoch J2000. Also, the planetocentric coordinate system is fixed, and each axis is pointing in the same direction as the ecliptic coordinate system. Figure 7 represents each coordinate system.

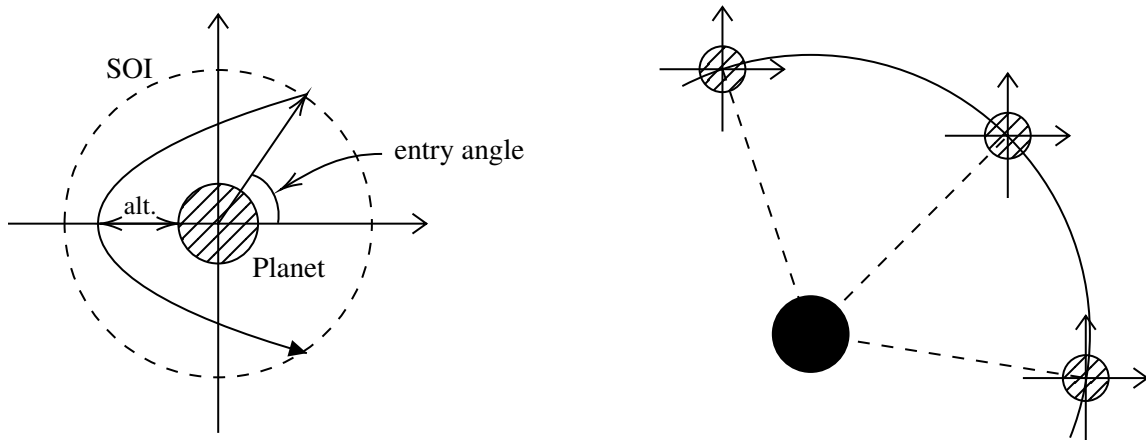


Figure 7: Visual description of terms and coordinate system

Entry Point Optimization

In order to find the optimal entry point for the highest Δv from free gravity assist, Lambert's problem is solved for all possible points around the boundary of the SOI. The results of all points are shown in Figures 8-10. From Figure 8, the minimum periapsis altitude of the spacecraft occurs for an SOI entry point at approximately 119° , however, the corresponding periapsis altitude is below 0 km. Figure 9 indicates that entry angles below 119° give negative Δv 's which are not valid. Finally, by evaluating Figure 10, the minimum altitude, 4179 km, for the maximum Δv , 5.377 km, can be found. Thus, from Figures 8-10, the best entry point is located at 120° . Since the best entry location to achieve the highest possible Δv can be selected from the listed criteria, this process can be automated by comparing the entry angle, periapsis altitude, and Δv .

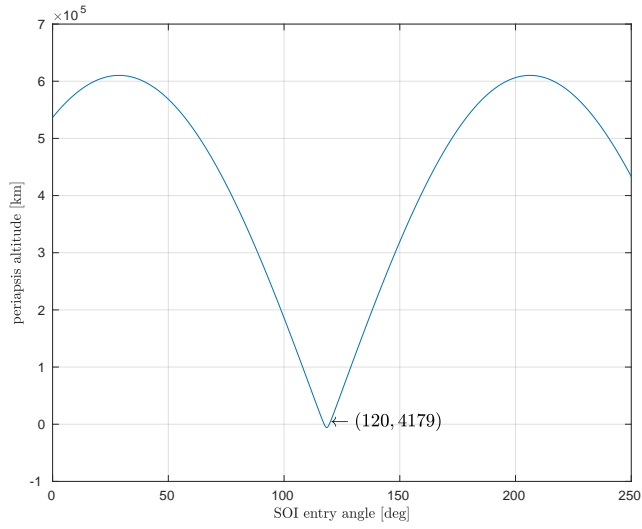


Figure 8: Periapsis altitude vs. entry angle of the free gravity assist maneuver

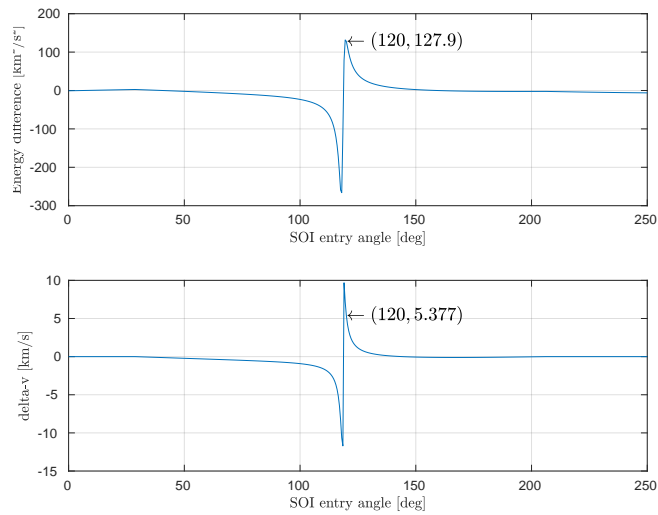


Figure 9: Specific energy and Δv vs. entry angle of the free gravity assist maneuver

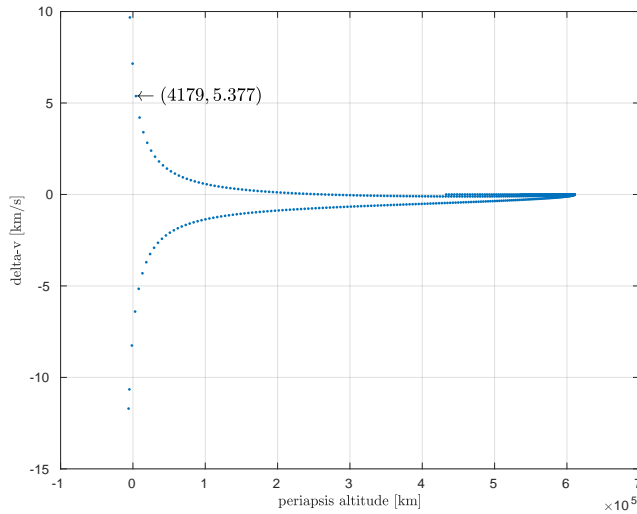
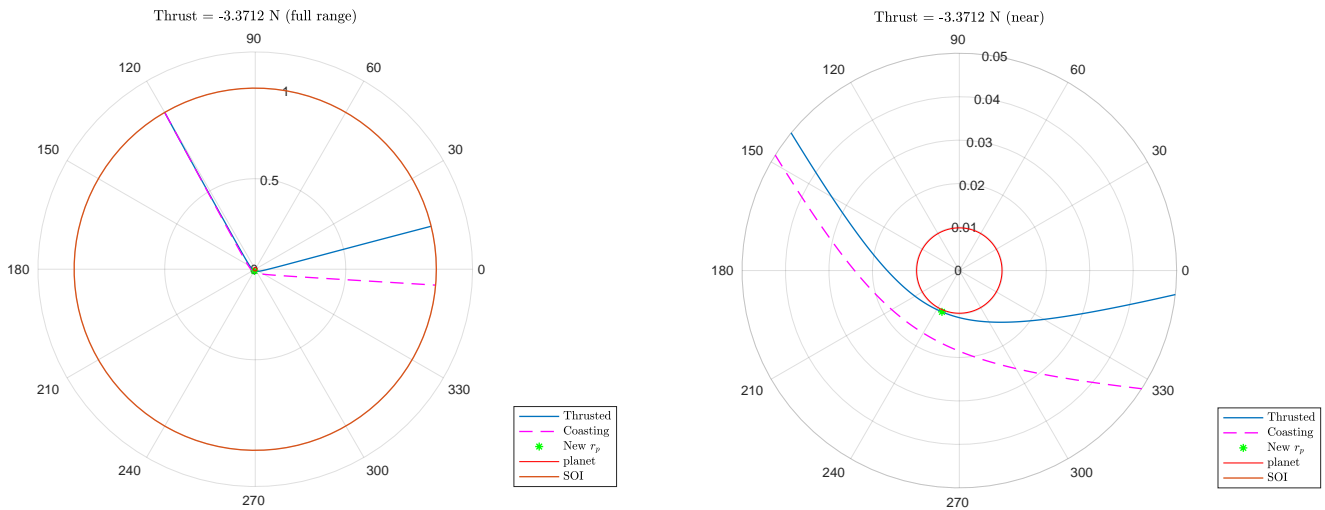


Figure 10: Δv vs. periapsis altitude of the free gravity assist maneuver

Thrust Application

Once the optimal entry location is defined, continuous thrust is applied to the spacecraft. In this work, the maximum thrust capability of the spacecraft is assumed to be 10 N. The PSO algorithm is used to find the optimal thrust for the maximum Δv gain. From the result of the PSO, the optimal thrust level is -3.37 N where the negative value represents a deceleration. The comparison of free and thrust gravity assist is shown in Table 1. As a result of the applied thrust, total Δv is increased by roughly 1.5 km/s, and the spacecraft approaches much closer to the planet.



(a) Free vs. thrust trajectory inside the SOI

(b) Free vs. thrust trajectory near the planet

Figure 11: Trajectory comparison of resulting trajectories with and without thrust method

The powered gravity assist around Venus changes the orbital characteristics. As shown in Table

	Free	Low Thrust
Thrust (N)	0	-3.371
Δv (km/s)	5.377	6.949
$\mathcal{E}_{\text{gain}}$ (km ² /s ²)	127.855	132.533
δ (deg)	58.175	73.727
Periapsis alt. (km)	4178.967	302.590
TOF (hours)	56.152	56.654

Table 1: Differences of Free and Low Thrust Gravity Assist

1, 132.5 km²/s² of specific energy is gained, and the orbit extends farther and closer to Mars' orbit. However, unlike the real Cassini mission, this work does not apply a trajectory correction maneuver. Since the adjustment is not made, the spacecraft is unable to encounter Venus again. The entire trajectory from Earth departure is plotted in Figure 12. Locations of Earth and Venus at

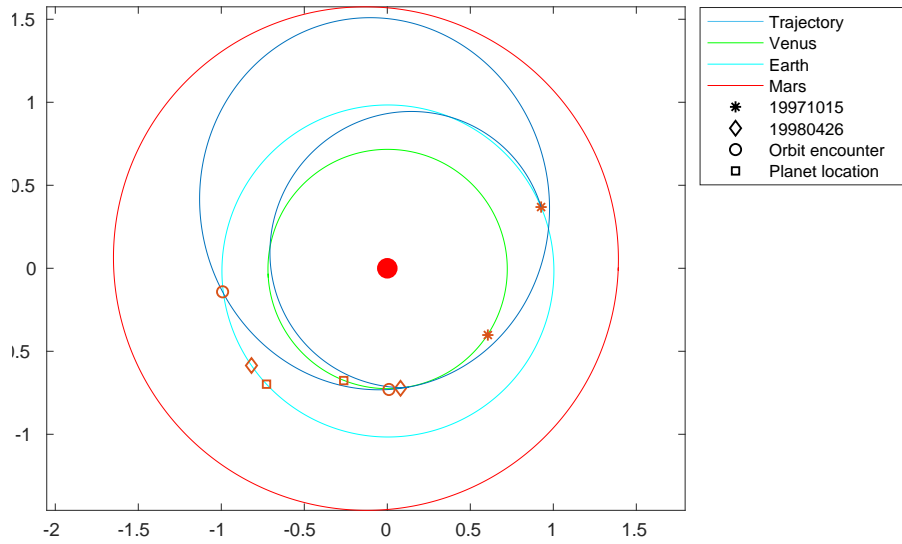


Figure 12: Preliminary result trajectory

departure (October 15, 1997) are marked as asterisks (*) and at arrival (April 26, 1998) as diamonds (◇). Circles (○) represent intersections of the spacecraft and planets' orbits. The actual locations of planets when the spacecraft is crossing planets' orbits are shown with squares (□). Thus, if the circle and square coincide on any planet's orbit, the spacecraft can make a gravity assist maneuver.

The preliminary results show that applied thrust can significantly boost the Δv gain from the gravity assist. Also, the radius of periapsis is clearly lowered as shown in Figure 11b. In order to clarify the influence of pure thrust versus lowering the periapsis altitude, let the periapsis location be the control variable while varying the entry location by 1 degree. The reason for using different entry points is because there is a unique path that can pass it from each entry location. Hypothetically, if thrust is the major factor that affects Δv gain, applying thrust should show improvement in Δv when periapsis is fixed. Thrust directions and magnitudes are chosen from the PSO algorithm. Since the goal of the PSO in this work it to maximize Δv , the resultant values are the best scenarios from given conditions. Table 2 compares results from 4 different test cases including the reference case which is the free gravity assist entering the SOI at 120°.

	119 deg	120 deg (Ref.)	121 deg	122 deg
Thrust (N)	4.09	0	-4.95	-8.46
Δv (km/s)	5.372	5.377	5.511	5.489
$\mathcal{E}_{\text{gain}}$ (km ² /s ²)	130.377	127.855	127.489	125.374
δ (deg)	54.574	54.965	56.695	56.794
Periapsis alt. (km)	4178.968	4178.968	4178.968	4178.968
TOF (hours)	55.850	56.152	56.999	57.183

Table 2: Comparison of different entry points

Figure 13 shows all compared trajectories. All of them pass the same periapsis location while using different amounts of thrust and leaving the SOI close to each other. From the results in Table 2, both Δv and specific orbital energy are not increased much or even decreased. It proves that applying thrust itself is not advantageous but flying closer to a planet can allow the spacecraft to maximize Δv gain from the gravity assist. Thus, to acquire the most gain from the gravity assist maneuver with continuous thrust, it is suggested to target the lowest possible periapsis altitude.

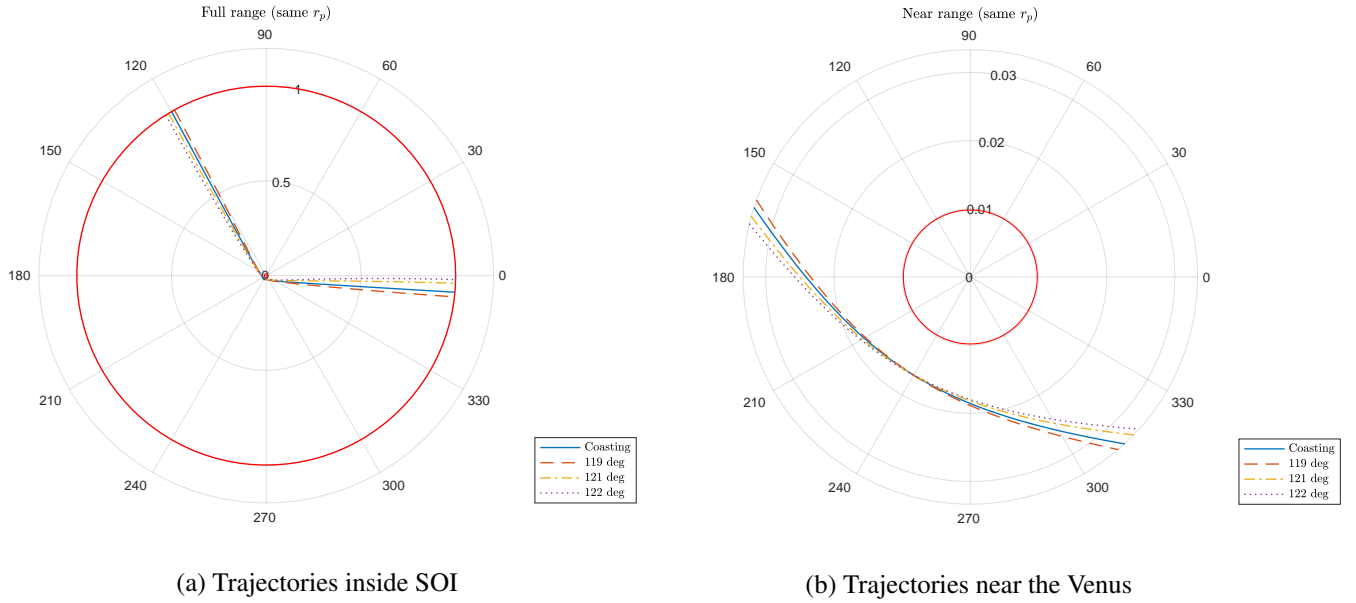


Figure 13: Comparison of paths inside SOI from different entry locations

CONCLUSION

A gravity assist strategy with continuous low thrust is presented in this work. The technique to find the trajectory for powered gravity assist is developed and tested. Also, potential methods to search for the multiple gravity assist sequence are discussed. The preliminary simulation is performed to reproduce the Cassini mission trajectory while not adopting a deep space maneuver after the first Venus flyby.

An increase in efficiency of gravity assist can be expected when low thrust is applied during the flyby. In the future, the main objective for the PSO can be modified from simply maximizing the

Δv gain to enough Δv to reach the next target planet in order to give flexibility. Then, a search sequence method can help complete the multiple gravity assist mission design.

Since the research is still in progress, the preliminary results presented have limitations that need to be improved for the future work. When the method is fully developed, it is hoped to automatically generate complete trajectories for low powered multiple gravity missions.

During the thrust maneuver, the spacecraft uses fixed direction and magnitude of propulsion to approach closer to the planet. The resulting thrust shown is decelerating the spacecraft for the entire period and possibly restricts potential Δv gain from the powered gravity assist. Instead, in the future, time-varying thrust direction and magnitude before and after passing the periapsis inside the SOI will be considered to further maximize Δv . Additionally, a new model for the thrust pointing angle could be developed for time-varying thrust pointing.

This preliminary work assumed a fixed spacecraft mass model which may not be realistic to simulate continuous thrust during the flyby. The mass flow rate from the spacecraft could be added to better model the dynamics.

NOTATION

$\mathcal{E}_{\text{gain}}$	specific energy gained after gravity assist maneuver
J	cost function
m	spacecraft mass
N_{GA}	total number of gravity assist maneuvers
N_{planets}	number of planets used for gravity assists
N_{thr}	thrust thrust magnitude
p_i	planet number ($i = 1, 2, \text{ and } 3$)
r	radial distance
r_a	radius of apoapsis
r_c	radius of circular orbit
r_p	radius of periapsis
T	thrust magnitude
t	time
v_c	circular orbit velocity
v_e	elliptical orbit velocity
v_r	radial velocity
v_θ	transverse velocity
\vec{x}	state vector
α	penalty multiplier
β	thrust pointing angle
β_i	polynomial coefficients of thrust pointing angle ($i = 1, \dots, 4$)
Δv	change in velocity before and after the maneuver
Δr_p	difference in periapsis distance
Δv_f	difference in final velocity (with and without thrust)
δ	turn angle
θ	angular displacement from x -axis
μ	standard gravitational parameter

REFERENCES

- [1] H. Oberth, “Ways to spaceflight,” techreport, NASA Techdocs, 1972.
- [2] A. F. S. Ferreira, A. F. B. A. Prado, and O. C. Winter, “A numerical mapping of energy gains in a powered Swing-By maneuver,” *Nonlinear Dynamics*, Vol. 89, No. 2, 2017, pp. 791–818, <https://doi.org/10.1007/s1107>.
- [3] A. F. B. d. Almeida Prado and G. d. Felipe, “An analytical study of the powered swing-by to perform orbital maneuvers,” *Advances in Space Research*, Vol. 40, No. 1, 2007, pp. 102–112, <https://doi.org/10.1016/j.asr.2007.04.09>.
- [4] M. Ceriotti and M. Vasile, “MGA trajectory planning with an ACO-inspired algorithm,” *Acta Astronautica*, Vol. 67, No. 9-10, 2010, pp. 1202–1217.
- [5] J. Englander, B. Conway, and T. Williams, “Automated Interplanetary Trajectory Planning,” *AIAA/AAS Astrodynamics Specialist Conference*, 2012.
- [6] D. H. Ellison, B. A. Conway, J. A. Englander, and M. T. Ozimek, “Analytic Gradient Computation for Bounded-Impulse Trajectory Models Using Two-Sided Shooting,” *Journal of Guidance, Control, and Dynamics*, Vol. 41, No. 7, 2018, pp. 1449–1462, 10.2514/1.G003077.
- [7] D. H. Ellison, B. A. Conway, J. A. Englander, and M. T. Ozimek, “Application and Analysis of Bounded-Impulse Trajectory Models with Analytic Gradients,” *Journal of Guidance, Control, and Dynamics*, Vol. 41, No. 8, 2018, pp. 1700–1714, 10.2514/1.G003078.
- [8] A. Gad and O. Abdelkhalik, “Hidden Genes Genetic Algorithm for Multi-Gravity-Assist Trajectories Optimization,” *Journal of Spacecraft and Rockets*, Vol. 48, No. 4, 2011, pp. 629–641.
- [9] M. Vasile and P. D. Pascale, “Preliminary Design of Multiple Gravity-Assist Trajectories,” *Journal of Spacecraft and Rockets*, Vol. 43, No. 4, 2006, pp. 794–805, 10.2514/1.17413.
- [10] D. Izzo, V. M. Becerra, D. R. Myatt, S. J. Nasuto, and J. M. Bishop, “Search space pruning and global optimisation of multiple gravity assist spacecraft trajectories,” *Journal of Global Optimization*, Vol. 38, June 2007, pp. 283–296.
- [11] S. Wagner and B. Wie, “Hybrid Algorithm for Multiple Gravity-Assist and Impulsive Delta-V Maneuvers,” *Journal of Guidance, Control, and Dynamics*, Vol. 38, Nov. 2015, pp. 2096–2107, 10.2514/1.G000874.
- [12] E. M. Standish, “Keplerian Elements for Approximate Positions of the Major Planets,” techreport, JPL/Caltech, N.D.
- [13] E. M. Standish and J. G. Williams, “Orbital Ephemerides of the Sun, Moon, and Planets,” Unpublished.
- [14] A. E. Bryson and Y.-C. Ho, *Applied Optimal Control*. Hemisphere, Washington, 1st ed., 1975.
- [15] B. A. Conway, ed., *Spacecraft Trajectory Optimization*. Cambridge, 2010.
- [16] K. W. Kloster, A. E. Petropoulos, and J. M. Longuski, “Europa Orbiter tour design with Io gravity assist,” *Acta Astronautica*, 2010.
- [17] N. J. Strange and J. M. Longuski, “Graphical Method for Gravity-Assist Trajectory Design,” *Journal of Spacecraft and Rockets*, Vol. 39, No. 1, 2002.
- [18] M. Okutsu and J. M. Longuski, “Mars Free Returns via Gravity Assist from Venus,” *Journal of Spacecraft and Rockets*, Vol. 39, No. 1, 2002, pp. 31–36, 10.2514/2.3778.
- [19] A. V. Labunsky, O. V. Papkov, and K. G. Sukhanov, *Multiple Gravity Assist Interplanetary Trajectories*. CRC Press, Nov. 1998.